Bulletin of the Geological Society of Malaysia 55 (2009) 73 – 79

Fractal and shape analyses of manganese dendrites on vein quartz

T. F. Ng* & G.H. Teh

Department of Geology, University of Malaya
50603 Kuala Lumpur, Malaysia
*Email address: thamfatt@gmail.com

Abstract— Manganese dendrites are common along joint planes in a quartz vein in Selayang, northern Kuala Lumpur. Individual dendrites mainly range from about 5 cm to 50 cm in length. They have variable shapes that range from simple shape with few branches to complex intricately branched patterns. Dendrites having different patterns may be found together along the same joint plane and some simple dendrites developed into more intricate forms. Digital photographs of dendrites were taken in the field and then converted to single bit images for fractal analysis. The images were also vectorised to measure the perimeter and area of the dendrites as well as the enclosing convex hull. These basic measurements were used to obtain the fractal dimension, lacunarity, PARIS factor, divergent ratio, fractal divergent ratio and fill factor for nine samples, which cover dendrites of various forms and complexities.

The fractal dimension of the dendrites measured using box counting algorithm ranges from 1.57 to 1.88. Generally, dendrites with broad and short branches have larger fractal dimension and those that have thin and long branches have smaller fractal dimension. Lacunarity and fill factor also show the same trend, while PARIS factor, divergent ratio and fractal divergent ratio values are higher in complex and intricately branched dendrites. There are dendrites with similar fractal dimension but have dissimilar patterns. At the same fractal dimension, the lacunarity is smaller for more complex and intricately branched dendrites, while the fractal divergent ratio is larger for dendrites with thinner branches. Although the values of both PARIS factor and divergent ratio increase with the increase in the intensity of branching, these parameters cannot be clearly related to the variation in the pattern of dendrites.

Keywords: Manganese dendrites, fractal dimension, lacunarity, shape factors

INTRODUCTION

Mineral dendrites with tree-like or fern-like growth patterns occur in all common rocks and minerals (Swartzlow, 1934). They are most commonly found on discontinuity planes such as joints, fractures and bedding. Manganese and iron dendrites are most commonly reported and studied (e.g. Potter & Rossman, 1979; Chopard *et al*., 1991; Garcia-Ruiz *et al*., 1994; Merdan & Bayirli, 2005).

The mineral dendrites are fractal objects, which look the same at whatever scale or scale-invariant (Mandelbrot, 1982, 1987). The geometry of fractals can be quantified by parameters such as fractal dimension (D), lacunarity (L) and connectivity (Q). Fractal dimension of manganese dendrites has been described in many literature (e.g. Vicsek, 1989; Chopard *et al*., 1991; Merdan & Bayirli, 2005), however, fractal dimension does not fully characterise the dendrite patterns. Dendrites having visually distinct patterns may have similar fractal dimension. Fractal dimension measures how much space is filled, while lacunarity measures how an object fills the space (Tolle *et al*., 2003). This paper characterises the pattern of manganese dendrites along joint planes in a vein quartz in Northern Kuala Lumpur using fractal dimension, lacunarity and other shape parameters such as PARIS factor, divergent ratio and fill factor.

GEOLOGY AND MORPHOLOGY

Manganese dendrites are well developed on joint planes of a large quartz vein in a granite quarry, in Selayang about 15 km north of Kuala Lumpur (Figures 1 and 2a). The quartz vein is striking at 120° and is mainly subvertical to steeply dipping to the northeast, but a section of the quartz vein exposed in the main quarry pit dips about 45° northeasterly. It is 5 m to 20 m thick and can be traced for about 2 km. The southwestern boundary between the quartz vein and granite is a fault contact and a 2 m thick fault breccia is found along this sinistral strike-slip fault (Figure 2b). The quartz vein is well jointed and the most distinct set is subparallel to the fault (Figure 2c).

Manganese dendrites occur in about 5% of the joint planes at the thicker section of the quartz vein exposed in the main quarry pit. Elsewhere along the quartz vein, the dendrites are less abundant. They often occur in clusters, where almost all the joints in a particular part of the quartz vein are ornamented with dendrites. The stems or main axes of growth of the dendrites are mainly subhorizontal and the orientations of the side branches are variable (Figure 2d). The dendrites are found on planar and stepped joint planes. The dendrites are quasi-two dimensional objects where their growth is restricted along the narrow joints. However, some dendrites are observed to grow along one joint plane and at the intersection with another joint, it bifurcates and continue to grow along both joint planes (Figure 3).

The size of individual manganese dendrites ranges from about 1 cm to about 2 m in length, and most are between 5 cm to 50 cm long. Some of the dendrites are intricately interconnected and it is not possible to separate one dendrite from another. The shape of the dendrites is variable. It ranges from simple lobate shape with few branches (Figure 4A) to

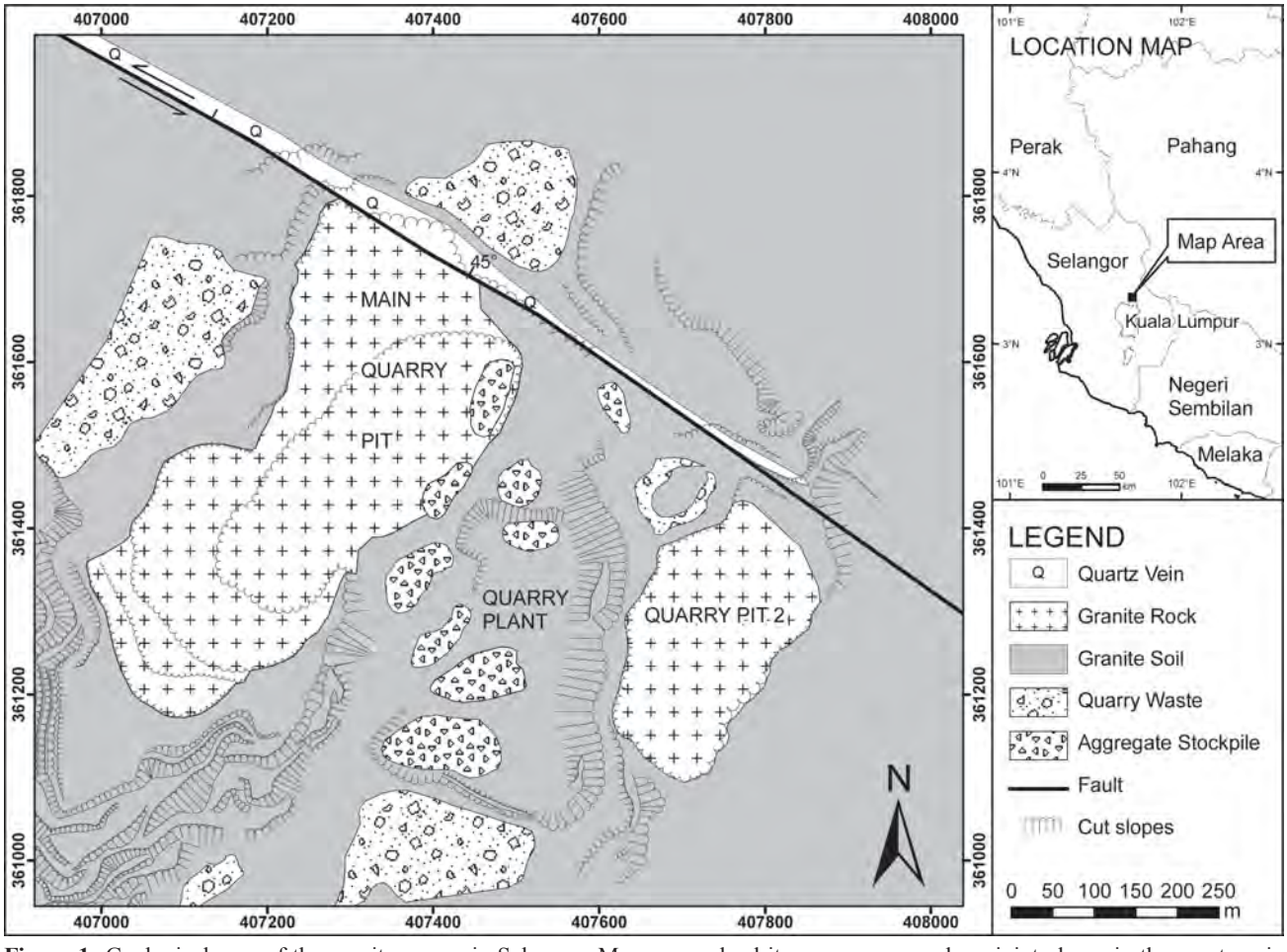

Figure 1: Geological map of the granite quarry in Selayang. Manganese dendrites are common along joint planes in the quartz vein cutting the granite.

Figure 2: A) Photograph of the quartz vein exposure along the northern face of the main quarry pit. B) A zone of fault breccia occurring along southwestern boundary between the quartz vein and granite. C) The quartz vein is well jointed and the most prominent joint set is subparallel to the vein and fault. D) Manganese dendrites with subhorizontal growth axis (arrow).

fern-like shape with many intricate broad branches (Figures 4B, 4C and 4D), and from simple blade-like structure that branches near the base (Figures 4E and 4I) to seaweed-like with many intricate long thin branches (Figures 4G and 4H). Not only that all these dendrites forms may be found together along the same joint plane, some simple dendrites developed into more intricate forms (Figure 5a).

Irregular and non-dendritic manganese deposits are also found on joints with larger aperture and on quartz crystals in vugs (Figure 5b). Some of the non-dendritic manganese deposit may develop into dendrites (Figure 5c). The branches of most of the manganese dendrites are not regularly spaced, although some fern-like dendrites have regularly spaced opposite branches. The thickness of the branches is variable. They may taper away from the base of growth (Figure 4H), become thicker (Figure 4B and 4I) or remains about the same thickness (Figure 4E). The ends of the branches are generally rounded.

MINERALOGY AND GROWTH MECHANISM

Manganese dendrites are formed by manganese oxide minerals and in the past have been mistakenly presumed to compose of pyrolusite (Potter & Rossman, 1979). Material forming manganese dendrite was scrapped off the vein quartz and crushed in an agate mortar. The sample was analysed using X-ray diffraction. Scanning was carried out from 3° to 60° 2θ at a goniometer speed of 2° 2θ per minute using CuKα radiation. However, no distinct peak was obtained. This indicates that the material forming the manganese dendrites is amorphous or have low crystallinity. Electronprobe microanalyser studies indicate that the dendrites are composed mainly of cryptomelane (KMn_8O_{16}).

Swartzlow (1934) suggested that dendrites are formed along joint planes by the distribution of suspended material due to surface tension of evaporating water and he managed to produce dendrites experimentally. However, according to Garcia-Ruiz *et al*. (1994), the evaporation mechanism cannot explain the observations they made on manganese dendrites. The evaporation mechanism also cannot explain the dominantly subhorizontal main growth axis of manganese dendrites along the joint planes observed in this study. If the dendrites were formed by evaporation on exposure to air at the surface, one would expect a subvertical growth axis.

The manganese dendrites are low crystallinity material and the overall growth pattern is not geometrically related to the crystal structure. This is typical of random dendritic fractal formed by an irreversible precipitation process occurring in conditions far from equilibrium (Vicsek, 1989). Two Laplacian growth processes have been proposed to explain the growth of dendrites. The first is diffusion-limited aggregation (DLA) model (Witten & Sander, 1983; Chopard *et al*., 1991) and the other is viscous fingering (VF) process (Maloy *et al*., 1985; Vicsek, 1989). DLA is the process whereby a fractal cluster is grown by allowing particles to undergo random walk due to Brownian motion until it hits any particle in the same cluster to form aggregates. This process has been widely studied using computer simulation. VF is a pattern created when a less viscous fluid displaces a more viscous fluid contained in a small gap between two glass plates (known as a Hele-Shaw cell). Both DLA and VF produce fractal growth patterns with the same fractal dimension of about 1.71 and are in the same universality class (Mathiesen *et al*, 2006). Observation of the manganese dendrites in this paper favours the formation by viscous fingering due to cyclic fluid flows and the details will be published elsewhere.

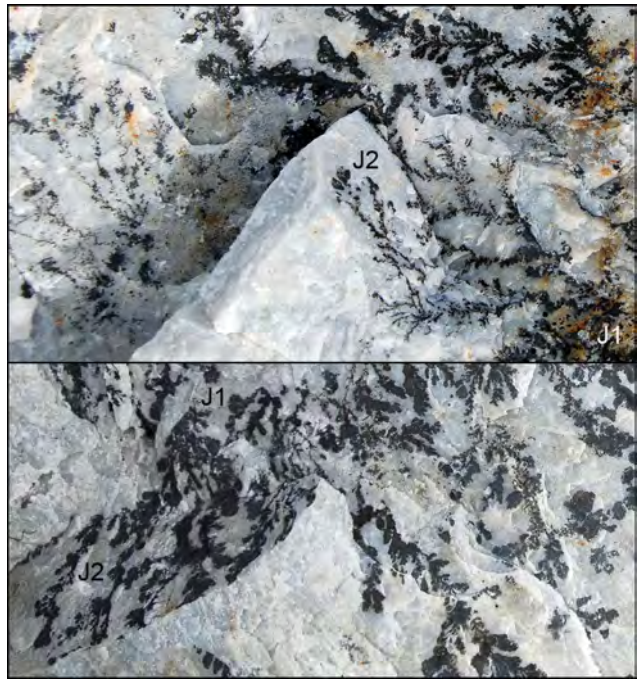

Figure 3: The manganese dendrites shown in the photographs initailly grow on joint J1, and at the intersection with joints J2 continue to grow on both joint planes.

MEASUREMENTS OF FRACTAL AND SHAPE FACTORS

Image preparation and basic measurements

The basic and fractal measurements as well as shape factors described in this paper are listed in Table 1. All the measurements were derived from 24 bit colour digital photographs or images of dendrites. The images were taken in the field using a digital single lens reflex camera (DSLR) with resolution of 4288 x 2848 pixels. Nine images covering dendrites of various forms and intricacies were chosen for the analysis of fractal geometry and related shape parameters. These images have high contrast where the black dendrites can be clearly differentiated from the white vein quartz. The images were cropped to isolate the dendrites. The cropped images were resized to a width of 1024 pixels by bicubic interpolation, giving final image resolution that ranges from 5.5 μm per pixel in sample DMn03 to 98 μm per pixel in sample DMn09. The resized images were then converted to 1 bit images. Fractal dimension and lacunarity were calculated from the single bit dendrite images. The

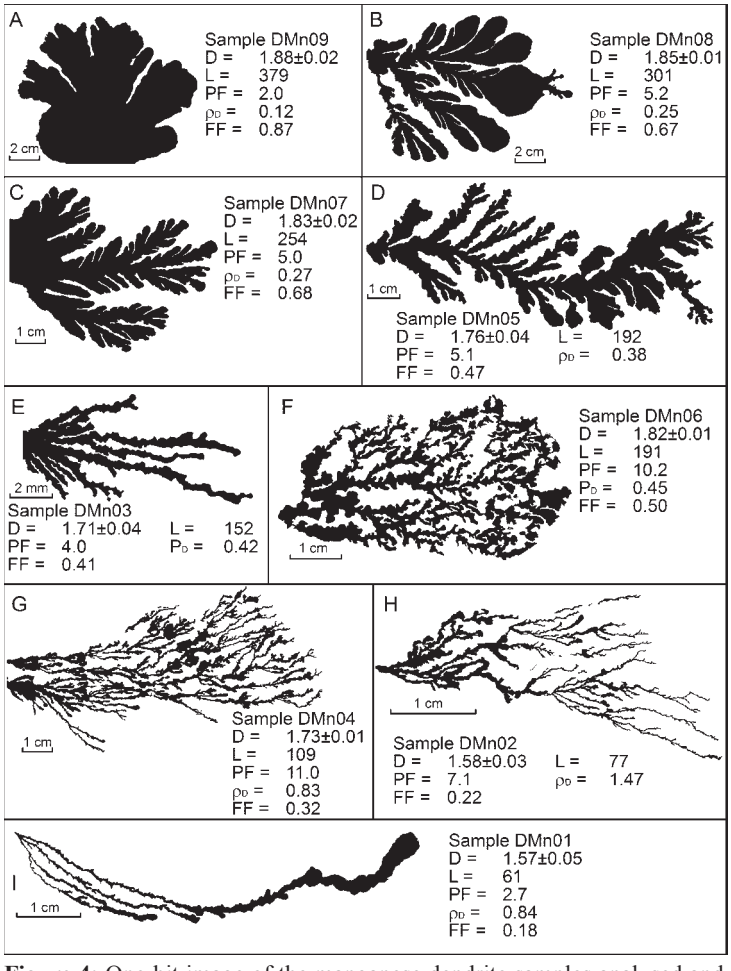

Figure 4: One-bit image of the manganese dendrite samples analysed and their fractal and shape parameters (see Table 1 for symbols used).

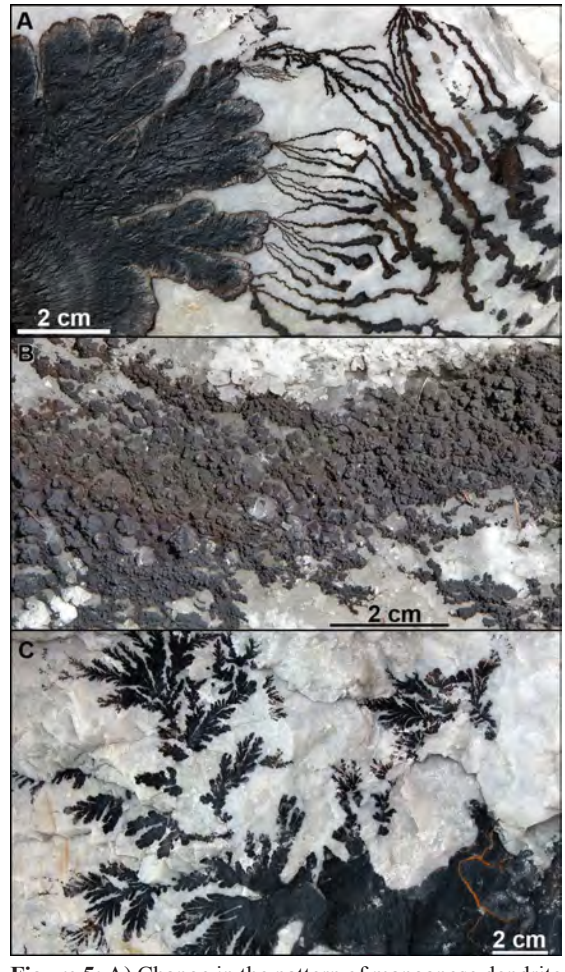

Figure 5: A) Change in the pattern of manganese dendrite during growth. The initial shape is broad with several short branches and it continued to grow into thin and long branches. B) Non-dendritic manganese oxide coating on quartz crystals in a vug. C) A non-dendritic manganese deposit (bottom right) developed into ferm-like dendrites.

Table 1: Definitions of measurement and shape factors used in this paper

Parameter	Symbol	Definition / Description
Basic measurements		
Perimeter	P	Length of original vectorised outline
Area	A	Area of original vectorised outline
Perimeter of convex hull	P_{CH}	Length of outline of convex envelope
Area of convex hull	A_{CH}	Area of convex envelope
Fractal measurements		
Fractal dimension	D	Fractal dimension calculated using box counting algorithm
Lacunarity	L	Lacunarity calculated using gliding box algorithm
Shape factors		
PARIS factor	PF	$= P / P_{CH}$
Divergent ratio	ρ	$= P / \sqrt{A}$
Fractal divergent ratio	ρ_D	$= P^{1/D} / \sqrt{A}$
Fill factor	FF	$= A/A_{CH}$

images of dendrites were vectorised to form polygons and have the length of their outline or perimeter and their area calculated using the geographical information system (GIS) software ArcGIS. A convex hull is constructed around each dendrite polygon and the perimeter and area of the convex hull are also calculated

Fractal dimension

Fractal dimension D was measured using box counting algorithm (Vicsek, 1989), which is the most common method to estimate fractal dimension. This method is implemented from the definition of fractal dimension shown below.

$$D = \lim_{\varepsilon \to 0} \log N(\varepsilon) / -\log \varepsilon$$

$N(\varepsilon)$ is the number of boxes or squares needed to cover the entire fractal object, ε is the size of the boxes. The estimation of D involves step-by-step iteration. After each step, ε is increased and $N(\varepsilon)$ is calculated for each step. The steps for box size used in this study follow a power of two (ε = 1, 2, 4, 16, … pixels). A plot of log $N(\varepsilon)$ versus

log ε is made and for fractal data sets, the relationship is linear and absolute value of the slope corresponds to D. Figure 6 shows the plot for one of the dendrites. The high coefficient of correlation of the plots ($r^2 > 0.9$) indicates that the dendrites are fractal structures. The accuracy of the calculation was verified by analysing a triadic Koch curve with D = ln4/ln3. The measured D value is 1.264 which is within 0.2% of the actual value.

Lacunarity

The gliding box algorithm (Plotnick *et a*l., 1996) was used for the calculation of lacunarity. This method is similar to the box counting method. A box size ε is chosen and the number of set pixels within it is counted. Counting is repeated where the box is centred, in turn, at each pixel within the image. A distribution of box masses $B(n,\varepsilon)$ is created where B is the number of boxes with n points and ε size. The distribution is converted into a probability distribution and lacunarity is estimated from the ratio between the second moment and square of first moment of the box mass probability distribution. Lacunarity calculation using gliding box algorithm is sensitive to the box mass (Tolle *et al*., 2003). This is shown in the plot of lacunarity against box size (Figure 7). To enable direct comparison of lacunarity between samples, all images used in the analysis were resized to a width of 1024 pixels.

Shape factors

A number of shape factors have been described (e.g. Barret, 1980; Drevin & Vincent, 2002; Heilbronner & Keulen, 2006; Al Rousan *et al*., 2007), which can be easily calculated from the perimeter and area of the objects. Most of these parameters were used to characterise particles in clastic rocks, sediments and crushed rocks, which have relatively simple shapes compared to the dendrites. Some of the shape factors that can be used to characterise the manganese dendrites are described below.

The PARIS factor (Panazzo & Hurlimann, 1983) is a measure for irregularity of grain boundary and is defined as the ratio of the perimeter divided by the outline of the convex hull that envelopes the grain. A smooth grain, a circle or any grains with convex outlines will have a PARIS factor of 1. The value increases as the grain boundary becomes irregular and lobate.

The divergent ratio ρ is the ratio between the perimeter and the square root of the enclosed area. For objects of the same shape, it is independent of the size of the objects (i.e. ρ for circle is 3.44, square 4.00 and equilateral triangle 4.56) and the value increases with the increase in complexity and angularity of the object outline. However, for fractal objects, the perimeter depends on the scale of measurement (length of yardstick). Mandelbrot (1983) shows that for fractal curves, the divergent ratio can be replaced by a modified fractal ratio ρ_D, where $\rho_D = (\text{Perimeter})^{1/D} / \text{Area}^{1/2}$. The fractal divergent ratio is independent of the size of the fractal objects but depends on the yardstick chosen.

Table 2: Results of the fractal geometry and shape factor measurements. See Table 1 for symbols used.

Sample	D	L	PF	ρ	ρ_D	FF
DMn01	1.57	60.9	2.7	33.4	0.84	0.18
DMn02	1.58	77.1	7.1	70.4	1.47	0.22
DMn03	1.71	151.9	4.0	26.0	0.42	0.41
DMn04	1.73	108.8	11.0	80.9	0.83	0.32
DMn05	1.76	192.2	5.1	32.0	0.38	0.47
DMn06	1.82	190.6	10.2	55.9	0.47	0.50
DMn07	1.83	254.2	5.0	22.9	0.27	0.68
DMn08	1.85	301.2	5.2	24.2	0.25	0.67
DMn09	1.88	379.0	2.0	8.0	0.12	0.87
Average	1.75	190.7	5.8	39.3	0.56	0.48

The fill factor FF measures how much the space is filled by an object. It is given by the ratio between the area of an object and the area of the convex hull. Similar to the PARIS factor, smooth grains, a circle or any grains with convex outlines will have a fill factor of 1. The value decreases as the grain boundary becomes irregular and less space is filled.

RESULTS AND DISCUSSION

The fractal dimension of the manganese dendrites calculated using box counting method has a narrow range from 1.57 to 1.88 and the average value is 1.75 (Table 2, Figures 4A to 4I). The values are similar to manganese dendrites on limestone (D=1.78) and quartz (D=1.51) reported by Chopard *et al*. (1991) and on magnesite ore (D=1.61–1.88, Merdan & Bayirli, 2005). Generally, dendrite with broad and short branches have larger fractal dimension compared to those with long and thin branches. However, samples DMn05 with rather broad fern-like pattern has relatively low fractal dimension, compared to sample DMn07, which has similar but shorter branches.

The lacunarity value has a broader range of between 61 and 379 (Table 2, Figures 4A to 4I). Manganese dendrite with broad and simple branches generally has larger lacunarity compared to those with long and thin branches. Generally, lacunarity increases with the increase in fractal dimension (Figure 8). Sample DMn04 deviate from this trend, where it has lower lacunarity (L=109, D=1.73) compared to sample DMn03 that has similar fractal dimension (L=152, D=1.71). Sample DMn06 (L=191, D=1.82) also has lower lacunarity than sample DMn07 (L=254, D=1.83) that has similar fractal dimension. It is observed that both dendrites with lower lacunarity have thinner and more complex branches compared to dendrites having similar fractal dimension but larger lacunarity.

The PARIS factor and divergent ratio measure the irregularity of the dendrites from their perimeter. The PARIS factor increases from 2 in sample DMn09 to 11 in sample DMn04 with the general increase in the intensity

of branching. This is expected as increase in branching will increase the length of the dendrite outlines. For example, samples DMn03 (D=1.71, PF=4.0) and DMn04 (D=1.73, PF=11.0) have similar fractal dimension, but the later which is intricately branched has larger PARIS factor value. Similar trend is shown by samples DMn07 (D=1.83, PF=5.0) and DMn06 (D=1.82, PF=10.2). Generally, the divergent ratio also increases with increase in the complexity and branching of the dendrites. However, changes in the value of both PARIS factor and divergent ratio cannot be clearly related to the variation of the dendrite patterns. This is probably because the perimeter is measured from images of the same size (width=1024 pixels) but not of the same scale or resolution. For fractal objects, it is not possible to obtain a specific value for the perimeter due to the presence of small indentations and it is important that comparison of shape factor that involves perimeter to be made at the same scale.

Compared to the divergent ratio, the relationship between the shape of the dendrites and the fractal divergent ratio is more clearly shown. Simple dendrite with broad branches has the lowest fractal divergent ratio and the value increases with the decrease in branch thickness (Figure 9). This is clearly shown by the sample pairs DMn01 and DMn02, DMn04 and DMn03, and DMn06 and DMn07. Each of these three pairs of samples have similar fractal dimension, but the dendrites with relatively thicker branches have greater fractal divergent ratios.

The fill factor of the manganese dendrites is greater for those with simple shapes with closely spaced or broad branches (eg. sample DMn09, FF=0.87), compared to dendrites with long, widely spaced and thin branches (eg. samples DMn02, FF=0.22; DMn01, FF=0.18). The fill factor shows significant positive correlations with both the fractal dimension and lacunarity (Figure 10).

CONCLUSION

Manganese dendrites of various patterns and sizes are found along joint planes in a quartz vein in Selayang, northern Kuala Lumpur. The patterns of the dendrites were characterised using fractal and shape analyses. The fractal dimension of the dendrites measured using box counting algorithm ranges from 1.57 to 1.88. Generally, dendrites with broad and short branches have larger values of fractal dimension, lacunarity and fill factor compared to those that have thin and long branches. The opposite trend is observed for PARIS factor, divergent ratio and fractal divergent ratio. There are dendrites with similar fractal dimension but have dissimilar patterns. At the same fractal dimension, the lacunarity is smaller for more complex and intricately branched dendrites, while the fractal divergent ratio is larger for dendrites with thinner branches.

ACKNOWLEDGEMENT

Financial assistance provided by University of Malaya (PJP289/2007C & RG045/09AFR) is greatly appreciated.

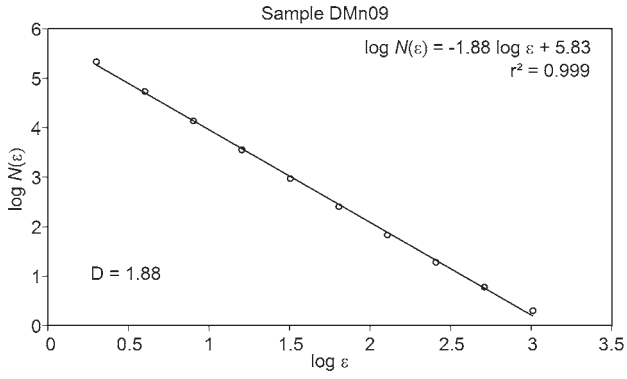

Figure 6: Plot of logarithm of number of boxes N(ε) required to cover the dendrite versus logarithm of box size ε for sample DMn09. Fractal dimension is obtained from the absolute value of the slope of the best fit line.

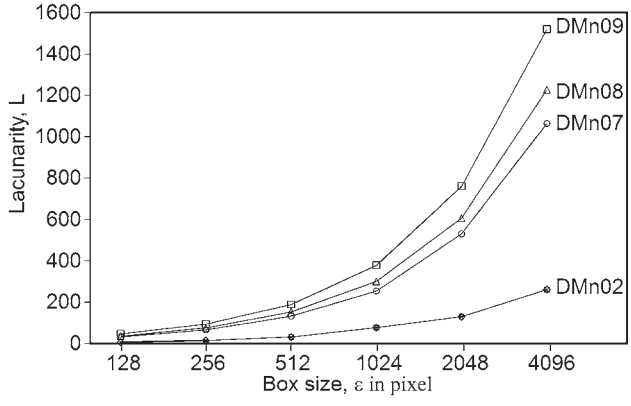

Figure 7: Plot of lacunarity calculated from dendrite images of various pixel sizes, for four dendrite samples.

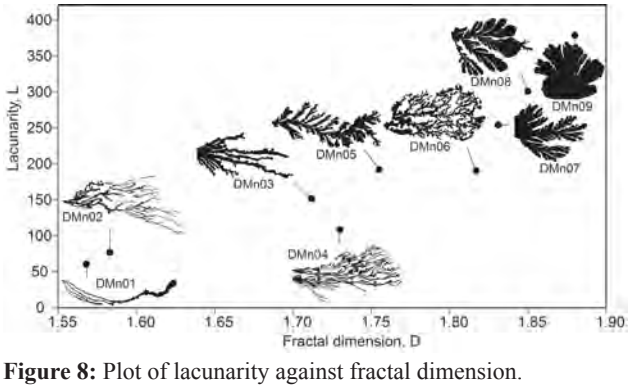

Figure 8: Plot of lacunarity against fractal dimension.

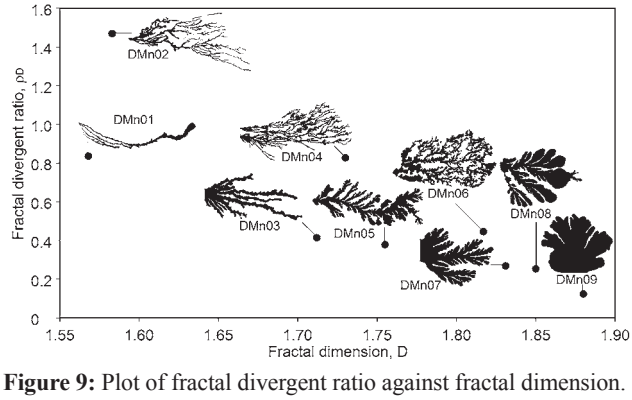

Figure 9: Plot of fractal divergent ratio against fractal dimension.

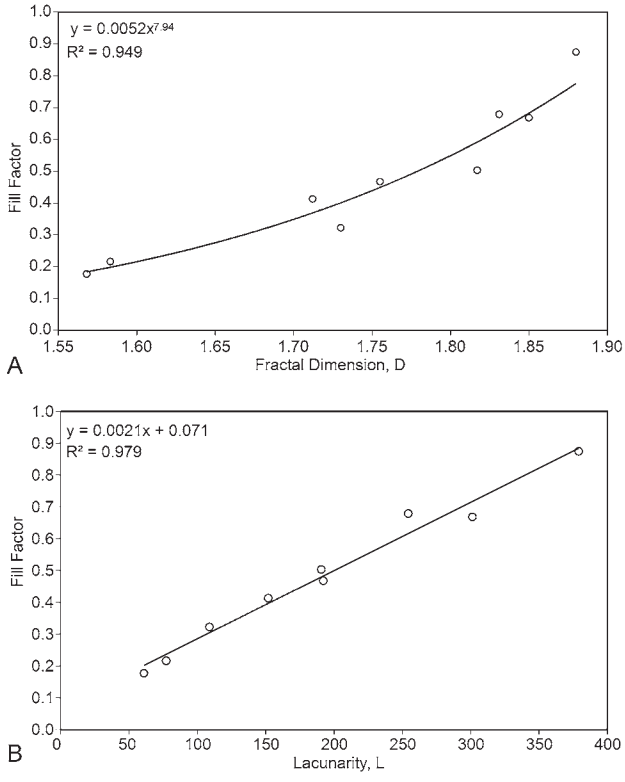

Figure 10: Plots of fill factor against fractal dimension (top) and lacunarity (bottom).

REFERENCES

Al-Rousan, T., Masad, E. Tutumluer, E. & Pan, T., 2007. Evaluation of image analysis techniques for quantifying aggregate shape characteristics. Construction and Building Materials 21: 978–990

Barret, P., 1980. The shape of rock particles, a critical review. Sedimentology, 27:291–303.

Chopard, B., Herrmann, H.J. & Viscek, T., 1991. Structure and growth mechanism of mineral dendrites. Nature, 353:409-412.

Drevin, G.R. & Vincent, L., 2002. Granulometric determination of sedimentary rock particle roundness. In: H. Talbot, R. Beare (Eds): Proceedings of ISMM2002, p. 315-325.

Garcia-Ruiz, J.M., Otalora, F., Sanchez-Navas, A. & Huges-Rolando, F.J., 1994. The formation of manganese dendrites as the mineral record of flow structure. In: Kruhl, J.H. (ed.) Fractals and Dynamic Systems in Geoscience. Springer-Verlag, Berlin, p. 307-318.

Heilbronner, R. & Keulen, N, 2006. Grain size and shape analysis of fault rocks. Tectonophysics, 427:199-216.

Maloy, K.J., Feder, J. & Jossang, T., 1985. Viscous fingering fractals in porous media. Physical Rev. Lett., 55:2688-2691.

Mathiesen, J., Procaccia, I, Swinney, H.L. & Thrasher, M., 2006. The universality class of difussion-limited aggregation and viscous fingering. Europhysics Lett., 76:257-263.

Mandelbrot, B.B., 1983. The Fractal Geometry of Nature. Freeman, San Francisco.

Mandelbrot, B.B., 1987. Fractals. Encyclopedia of Physical Science and Technology 5:579-593.

Merdan, Z. & Bayirli, M., 2005. Computation of the fractal pattern in manganese dendrites. Chinese Physical Letter, 22(8):2112-2115.

Panazzo, R. & Hurlimann, H., 1983. A simple method for the quantitative discrimination of convex-concave lines. Microscopica Acta, 87:169-176.

Plotnick, R.E., Gradner, R.H., Hargrove, W.W., Prestegaard, K. & Perlmutter, M. 1996. Lacunarity analysis: A general technique for the analysis of spatial patterns. Physical Rev. E, 53:5461-5468.

Potter, R.M. & Rossman, G.R., 1979. Mineralogy of manganese dendrites and coatings. American Mineralogist, 64:1219-1226.

Swatzlow, C.R., 1934. Two dimensional dendrites and their origin. American Mineralogist, 19:403-411.

Tolle, C.R., McJunkin, T.R., Rohrbaugh, D.T. & LaViolette, R.A., 2003. Lacunarity definition for ramified data sets based on optimal cover. Physica D, 179:129-152.

Vicsek, T., 1989. The Fractal Growth Phenomena. World Scientific, Singapore, 488 p.

Witten, T.A. & Sander, L.M., 1983. Diffusion limited aggregation. Physical Review B, 27:5686-5697.

Manuscript received 6 November 2008
Revised manuscript received 17 April 2009